Photon conversion processes in dispersive microcavities: Quantum-field model

Alex Hayat and Meir Orenstein*
Department of Electrical Engineering, Technion, Haifa 32000, Israel
(Received 20 July 2007; published 28 January 2008)

We present a simple quantum-field model for photon frequency conversion processes in dispersive dielectric microcavities, allowing practical calculations of conversion rates and efficiency optimization. The model incorporates the effect of dispersion into the structure of spatial cavity eigenmodes, while the material nonlinear properties enter the calculations through the coupling coefficients. Similar to the radiative atomic transitions, cavity photon-to-photon decay rates are derived for stimulated and spontaneous photon conversion. The phase matching requirement for a nonlinear process in a cavity is shown to be translated into a nonlinear mode overlap, manifesting the momentum conservation in a k space spanned by the cavity eigenmodes. We illustrate the efficiency of the model by calculating degenerate two-photon and three-photon parametric down-conversion rates and analyze the photon lifetime dependence on various cavity and material parameters.

DOI: 10.1103/PhysRevA.77.013830 PACS number(s): 42.60.Da, 42.50.Dv, 42.65.Lm

I. INTRODUCTION

The nonlinear-optical process of spontaneous parametric down-conversion (SPDC) provides a source of time-correlated photons enabling the construction of on-demand single-photon states [1–3] for security-proven quantum cryptography and higher photon-number states [4–6] for quantum computation and for fundamental physics research [7,8]. Furthermore, SPDC has been shown to generate efficiently entangled-photon states [9,10] required for many applications of quantum-information processing [11–14] and allowing practical tests of the foundations of quantum mechanics versus the local realism of classical physics [15]. Entangled photon pairs created via second-order nonlinearity $\chi^{(2)}$ have been demonstrated to violate Bell's inequalities for the statistical predictions of the theory [16], whereas three-photon Greenberg-Horne-Zelinger (GHZ) states, which can be created by third-order nonlinearity $\chi^{(3)}$ [17–19], violate the local realism even stronger by definite nonstatistical contradictions of quantum mechanical versus classical predictions [20].

In most of the nonlinear optics experiments including SPDC, material dispersion is usually compensated by birefringent crystal phase-matching [1–3,9–11] or quasi-phase-matching (QPM) in periodically poled ferroelectric crystals [21], where $\chi^{(2)}$ is spatially modulated with a period shorter than the nonlinear process coherence length L_c. Semiconductors offer a promising alternative due to their high nonlinear susceptibilities and compatibility with the existing photonic-circuit technology [22]. The main limitation of semiconductor materials, however, is their optical isotropy, which inhibits its natural birefringent phase matching, whereas implementations of QPM techniques in semiconductors [23] appear to be difficult.

A different concept of dielectric cavity nonlinear optics was recently proposed for materials which cannot be phase-matched by conventional means. A properly designed cavity with length shorter than L_c was shown to provide significant nonlinear process efficiency in integrated semiconductor microcavities by phase-matching traveling waves with dispersive mirror design [24] or using ring microresonators [25]. Moreover, high quality factor cavities can enhance the efficiency by raising the input field amplitudes, serve as storage for the produced photons and generate time-separation between exiting photons for photon-number-resolved detection [6,26]. Although stimulated photon conversion processes like second harmonic generation (SHG) and sum-frequency generation can be described by classical nonlinear optics, spontaneous nonlinear processes such as SPDC require a full quantum-field treatment. Field quantization procedure in homogeneous [27] and inhomogeneous dielectric structures including cavities [28] was rigorously developed previously following a Lagrangian-based formalism for dispersive linear dielectrics, whereas nonlinearities were sometimes introduced into field quantization for plane wave solution of the field [29–31]. Combining dielectric cavities, dispersion and nonlinear interactions into a rigorous quantum-field theory of dispersive cavity nonlinear process applicable to spontaneous photon conversion proved difficult, and a simpler model allowing practical calculations of conversion rates and efficiency optimization is required.

In this paper we develop a phenomenological quantum-field model for the nonlinear process of photon frequency conversion in dispersive dielectric cavities. The effect of dispersion is incorporated into the structure of spatial cavity eigenmodes, while the material properties enter the calculations only through the dielectric constant spatial dependence $\varepsilon(r)$ and the nonlinear coupling coefficients $\chi^{(2)}$ and $\chi^{(3)}$. The coupling between photon modes in the cavity is similar to atomic radiative transitions and thus simple expressions for photon-to-photon decay rates can be extracted for cavity SPDC. We validate the quantum model by comparing the stimulated SHG in the high-photon number limit to the classical time-dependent calculation according to the correspondence principle, where the slow time-varying envelope approximation is equivalent to the time-dependent perturbation theory assumptions in the quantum-field calculation. In a cavity nonlinear process the phase-matching requirement is translated to the optimization of a nonlinear mode overlap manifesting the momentum-conservation in a k space

*meiro@ee.technion.ac.il

 ©2008 The American Physical Society

spanned by the cavity modes. We employed this formalism to analyze the two-photon parametric down conversion (2PDC) and the three-photon parametric down-conversion (3PDC) rates in a dispersive cavity, where for concreteness the material properties are determined by a discrete-level atomic system.

The paper is organized as follows. In Sec. II a classical model for cavity nonlinear process is demonstrated assuming a slow time-varying envelope approximation for a weak nonlinear interaction using a specific example of SHG. In Sec. III a quantum-field phenomenological model is developed and its results for SHG are compared to the classical calculations in the strong field limit. In Sec. IV the model is applied to the calculation of the conversion rates for the spontaneous processes of 2PDC and 3PDC comparing the efficiency of the both. In Sec. V a particular example of a material with discrete atomic levels is analyzed and cavity optimization considerations are shown.

II. CLASSICAL MODEL FOR CAVITY NONLINEAR OPTICS—SHG

In contrast to the usual approach of traveling-wave interaction, our model is based on the interaction between spatial cavity standing-wave eigenmodes using the slowly time-varying envelope approximation. The following model deals with high-finesse cavities in which the allowed frequencies comprise a discrete set. Therefore, all the nonlinear interactions described here occur only for these allowed standing-wave cavity eigenmodes, which make up a complete set of wave equation solutions in a given cavity. Wave equation in a lossless, isotropic nonlinear dielectric with the nonlinear polarization $\tilde{P}_{\mathrm{NL}}$ as a radiation source is [32]

$$\nabla^2\tilde{E}(\mathbf{r},t)=\mu\varepsilon\frac{\partial^2\tilde{E}(\mathbf{r},t)}{\partial t^2}+\mu\frac{\partial^2\tilde{P}_{\mathrm{NL}}(\mathbf{r},t)}{\partial t^2}. \tag{1}$$

For the simplest second order $\chi^{(2)}$ nonlinear interaction of SHG $\tilde{P}_{\mathrm{NL}}(\mathbf{r},t)=(\chi^{(2)}/2)[\tilde{E}_1(\mathbf{r},t)]^2$, and the wave equation is

$$\nabla^2\tilde{E}_2(\mathbf{r},t)=\mu\varepsilon\frac{\partial^2\tilde{E}_2(\mathbf{r},t)}{\partial t^2}+\frac{\chi^{(2)}}{2}\frac{\partial^2[\tilde{E}_1(\mathbf{r},t)]^2}{\partial t^2}, \tag{2}$$

where $\tilde{E}_1(\mathbf{r},t)$ and $\tilde{E}_2(\mathbf{r},t)$ are the pump and the SH fields, respectively. Using $\omega_2=2\omega_1$ the pump and the second harmonic (SH) fields are

$$\tilde{E}_1(\mathbf{r},t)=E_1(t)e^{i\omega_1 t}F_1(\mathbf{r}),$$

$$\tilde{E}_2(\mathbf{r},t)=E_2(t)e^{i\omega_2 t}F_2(\mathbf{r}), \tag{3}$$

where $F_i(\mathbf{r})$ are the complete orthonormal set of spatial cavity eigenmodes, assumed to be unaffected by the weak nonlinear interaction, and $E_i(t)$ are the slowly time-varying envelopes relative to the oscillation period $T=2\pi/\omega$. Hence, the interaction-induced amplitude change rate ω_{int} is much smaller than the oscillation frequency ω:

$$\omega_{\mathrm{int}}=\frac{1}{E(t)}\frac{\partial E(t)}{\partial t}\ll\omega. \tag{4}$$

Assuming a strong undepleted pump $E_1(t)$ tuned to the cavity eigenmode frequency ω_1, for a cavity with an eigenmode at $\omega_2=2\omega_1$ as well, the wave equation is

$$E_2(t)e^{i\omega_2 t}\nabla^2F_2(\mathbf{r})=\mu\varepsilon_2\left[2i\omega_2\frac{\partial E_2(t)}{\partial t}-\omega_2^2E_2(t)\right]e^{i\omega_2 t}F_2(\mathbf{r})-\mu\frac{\chi^{(2)}}{2}\omega_2^2E_1^2(t)e^{i\omega_2 t}F_1^2(\mathbf{r}). \tag{5}$$

To calculate the time dependence of the SHG mode the equation is multiplied by $F_2^*(\mathbf{r})$ and spatially integrated yielding

$$\frac{\partial E_2(t)}{\partial t}=\frac{1}{2i}\left[\frac{\int d\mathbf{r}\,F_2^*(\mathbf{r})\nabla^2F_2(\mathbf{r})}{\mu\varepsilon_2\omega_2}+\omega_2\right]E_2(t)+\frac{i\gamma_2\chi^{(2)}\omega_2}{4\varepsilon_2}E_1^2(t), \tag{6}$$

where γ_2 is the three-mode nonlinear overlap

$$\gamma_2=\int d\mathbf{r}\,F_2^*(\mathbf{r})F_1^2(\mathbf{r}). \tag{7}$$

The first term on the right-hand side of Eq. (6) represents the radiative cavity losses of the $F_2(\mathbf{r})$ mode. For a very high-Q cavity, most of F_2 has an oscillatory behavior and thus

$$\nabla^2F_2(\mathbf{r})\approx-k^2F_2(\mathbf{r})=-\mu\varepsilon_2\omega_2^2F_2(\mathbf{r}) \tag{8}$$

and the loss term vanishes as expected for a very high-Q cavity. Equation (6) becomes

$$\frac{\partial E_2(t)}{\partial t}=\frac{i\gamma_2\chi^{(2)}\omega_2}{4\varepsilon_2}E_1^2(t). \tag{9}$$

The time dependence of the slow envelope SH field at undepleted pump is

$$E_2(t)=\int_0^t\frac{i\gamma\chi^{(2)\omega_2}}{4\varepsilon_2}E_1^2(t)dt'=\left[\frac{i\gamma_2\chi^{(2)}\omega_2}{4\varepsilon_2}E_1^2(t)\right]t. \tag{10}$$

The total energy stored in the SH field of a quasimonochromatic harmonic wave [33] is given by

$$U_2(t)=\varepsilon_2|E_2(t)|^2=\frac{1}{\varepsilon_2}\left|\frac{\gamma_2\chi^{(2)}\omega_2}{4}E_1^2\right|^2t^2=\frac{1}{\varepsilon_2}\left|\frac{\gamma_2\chi^{(2)}\omega_2}{4\varepsilon_1}U_1\right|^2t^2. \tag{11}$$

The quadratic time divergence of the SH energy [Eq. (11)] should be eliminated in a realistic cavity due to cavity loss or pump depletion and a certain steady state energy level would be established. Designating the cavity loss term by $-(\alpha/2)E_2(t)$, Eq. (6) becomes

$$\frac{\partial E_2(t)}{\partial t} = \frac{i\gamma\chi^{(2)}\omega_2}{4\varepsilon_2}E_1^2(t) - \frac{\alpha}{2}E_2(t). \tag{12}$$

Applying zero initial condition for the SH field, the $E_2(t)$ envelope time dependence (for a constant pump) is

$$E_2(t) = \frac{i\gamma\chi^{(2)}\omega_2}{2\varepsilon_2\alpha}E_1^2\left(1 - e^{-\frac{\alpha}{2}t}\right) \tag{13}$$

and at steady state, the pump P_1 and the SH P_2 powers are related by

$$P_2 = \frac{1}{\varepsilon_2\varepsilon_1^2}\left|\frac{\gamma\chi^{(2)}\omega_2}{2\alpha}\right|^2 P_1^2. \tag{14}$$

Hence in a properly designed cavity, with a large spatial mode overlap γ and small cavity loss term α, the nonlinear process efficiency can be enhanced significantly, regardless of the device dimensions, which can be as small as a few optical wavelengths.

III. QUANTUM FIELD MODEL FOR CAVITY NONLINEAR OPTICS—SHG

Our quantum model for cavity nonlinear-optical interaction is somewhat analogous to the description of atomic radiative transitions, thus enabling the calculation of photon-to-photon conversion rates. In this model only the radiation field is quantized as photons, whereas the matter is continuous, entering the equations only through the $\varepsilon(r)$ geometry while the nonlinear susceptibility serves as the coupling constant of the photon-photon interaction. The quantization of the field is based on the classical EM field Hamiltonian [27,30]:

$$H_{\text{tot}} = \int d\mathbf{r}\, \tilde{D}(\mathbf{r},t)\cdot\tilde{E}(\mathbf{r},t) = \int d\mathbf{r}[\varepsilon_0\tilde{E}(\mathbf{r},t) + \tilde{P}(\mathbf{r},t)]\cdot\tilde{E}(\mathbf{r},t)$$
$$= H_0 + H_{\text{int}}, \tag{15}$$

where the second order nonlinearity Hamiltonian in the interaction picture is

$$H_{\text{int}} = \frac{\chi^{(2)}}{2}\int d\mathbf{r}\, \tilde{E}_1(\mathbf{r},t)\tilde{E}_2(\mathbf{r},t)\tilde{E}_3(\mathbf{r},t). \tag{16}$$

With no interaction, the free field wave equation for a harmonic quasimonochromatic field is

$$\nabla^2 E(\omega) + \omega^2\mu\varepsilon(\mathbf{r},\omega)E(\omega) = 0. \tag{17}$$

According to this field equation of motion, the dielectric constant $\varepsilon(\mathbf{r},\omega)$ determines the eigenmodes including dispersion effects incorporating effectively all the quantum-electrodynamical interaction of the photons with the material. Thus the field solutions are

$$\tilde{E}(\mathbf{r},t) = \sum_k E_k F_k(\mathbf{r})e^{-i\omega_k t} + \text{c.c.}, \tag{18}$$

where E_k are the mode amplitudes and $F_k(\mathbf{r})$ is the complete set of orthonormal modes, which can be plane waves in free space or localized modes in a cavity. After quantization the field operator is

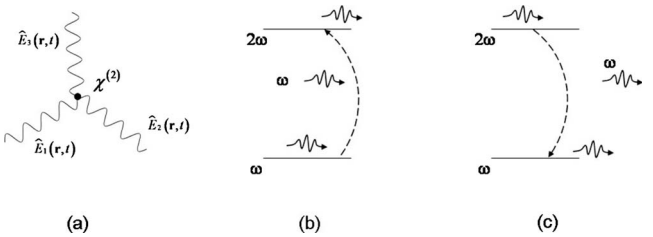

FIG. 1. (a) Three-photon vertex diagram for second-order nonlinear interaction. (b) Photon up-transition by one photon absorption—SHG. (c) Photon down-transition by one photon emission—2PDC.

$$\hat{E}(\mathbf{r},t) = \sum_k \sqrt{\frac{\hbar\omega_k}{\varepsilon_k}}[\hat{a}_k F_k(\mathbf{r})e^{-i\omega_k t} + \hat{a}_k^\dagger F_k^*(\mathbf{r})e^{i\omega_k t}], \tag{19}$$

where ε_k is the spatial average over $\varepsilon(\mathbf{r},\omega)$ for the $F_k(\mathbf{r})$ mode.

The interaction Hamiltonian density

$$\hat{\mathcal{H}}_{\text{int}} = \frac{\chi^{(2)}}{2}\hat{E}_1(\mathbf{r},t)\hat{E}_2(\mathbf{r},t)\hat{E}_3(\mathbf{r},t) \tag{20}$$

can be visualized employing the Feynman diagram method as a three-photon interaction vertex [Fig. 1(a)]. For a weak interaction (small enough $\chi^{(2)}$) the first order in the perturbation theory is a good approximation with

$$H_{\text{int}} \ll H_0 \Rightarrow \omega_{\text{int}} \ll \omega, \tag{21}$$

which is equivalent to the slow envelope approximation in the classical calculation [Eq. (4)].

Scattering matrix S to the first order in the perturbation theory is given by [34]

$$S^{(1)}(t) = \frac{-i}{\hbar}\int_0^t dt' H_{\text{int}}$$
$$= \frac{-i\chi^{(2)}}{2\hbar}\int_0^t dt' \int d\mathbf{r}\, \hat{E}_1(\mathbf{r},t)\hat{E}_2(\mathbf{r},t)\hat{E}_3(\mathbf{r},t). \tag{22}$$

In a process of SHG two pump photons are annihilated and one second-harmonic photon is created. Hence the initial and the final states are

$$|i\rangle = |n_{\omega_1}, 0_{\omega_2}\rangle,$$

$$|f\rangle = |n-2_{\omega_1}, 1_{\omega_2}\rangle, \tag{23}$$

with n being the number of photons in the pump field, where the cavity is designed to have resonant frequencies at ω_1 and $\omega_2 = 2\omega_1$. This process can be viewed as a transition of a photon from lower cavity eigenstate ω_1 to a higher state $2\omega_1$ by absorbing a ω_1 photon [Fig. 1(b)]. For SHG the only nonvanishing operator part of $S^{(1)}$ is $a_\omega a_\omega a_{2\omega}^\dagger$ leaving

$$S_{fi(t)} = \frac{-i\chi^{(2)}}{2\hbar}\sqrt{\frac{\hbar\omega_2}{\varepsilon_2}}\left(\frac{\hbar\omega_1}{\varepsilon_1}\right)\int_0^t dt' \int d\mathbf{r}\sqrt{n(n-1)} \times F_1(\mathbf{r})F_1(\mathbf{r})F_2^*(\mathbf{r})e^{-2i\omega_1 t'}e^{i\omega_2 t'}. \quad (24)$$

For a weak long-time interaction $(t\to\infty)$ the amplitude is

$$S_{fi} = \frac{-i\chi^{(2)}}{2\hbar}\sqrt{\frac{\hbar\omega_2}{\varepsilon_2}}\left(\frac{\hbar\omega_1}{\varepsilon_1}\right)\gamma_2\sqrt{n(n-1)}\delta(2\omega_1-\omega_2), \quad (25)$$

where the delta term stands for energy conservation and the spatial overlap γ_2 [Eq. (7)] is equivalent to the phase matching or the nonlinear mode overlap term in the classical analysis, which for a plane wave solution yields the usual delta term of linear momentum conservation:

$$\gamma_2^{\text{plane wave}} = \int d\mathbf{r}\, e^{2ik_1\mathbf{r}}e^{-ik_2\mathbf{r}} = \delta(2k_1-k_2). \quad (26)$$

The transition probability amplitude for finite $t<\infty$ is

$$P_{fi}(t) = S_{fi}(t)^2 = \left(\frac{\hbar\omega_2}{\varepsilon_2}\right)\left(\frac{\hbar\omega_1}{\varepsilon_1}\right)^2\left|\frac{\chi^{(2)}}{2\hbar}\gamma_2\right|^2 n(n-1) \times\left|\frac{e^{i\Delta\omega t}-1}{\Delta\omega t}\right|^2 t^2 \quad (27)$$

with $\Delta\omega=\omega_2-2\omega_1$. For a weak pump and long interaction time using the energy conservation restriction $\Delta\omega=0$ the probability is

$$P_{fi}(t) = \frac{\pi}{8\omega_2}\left(\frac{\hbar\omega_2}{\varepsilon_2}\right)\left(\frac{\hbar\omega_1}{\varepsilon_1}\right)^2\left|\frac{\chi^{(2)}}{2\hbar}\gamma_2\right|^2 n(n-1)t \quad (28)$$

emphasizing that, in contrast to the classical description of SHG, one photon cannot be up-converted. The corresponding transition rate is thus

$$R_{fi}(t) = \frac{P_{fi}(t)}{t} = \frac{\pi}{8\omega_2}\left(\frac{\hbar\omega_2}{\varepsilon_2}\right)\left(\frac{\hbar\omega_1}{\varepsilon_1}\right)^2\left|\frac{\chi^{(2)}}{2\hbar}\gamma_2\right|^2 n(n-1) \quad (29)$$

In most cases the SHG process includes two strong input pump fields and the case of a short-time interaction should be considered. For a stronger short-time interaction and $\Delta\omega=0$ the transition probability amplitude is

$$S_{fi}(t) = \frac{-i\chi^{(2)}}{2\hbar}\sqrt{\frac{\hbar\omega_2}{\varepsilon_2}}\left(\frac{\hbar\omega_1}{\varepsilon_1}\right)\gamma_2\sqrt{n(n-1)}\int_0^t dt' \quad (30)$$

and the corresponding transition probability is

$$P_{fi}(t) = S_{fi}^2(t) = \left(\frac{\hbar\omega_2}{\varepsilon_2}\right)\left(\frac{\hbar\omega_1}{\varepsilon_1}\right)^2\left|\frac{\chi^{(2)}}{2\hbar}\gamma_2\right|^2 n(n-1)t^2. \quad (31)$$

For high pump intensity and thus in a large photon number limit $n_{\omega 1}\to\infty$, the transition rate is

$$R_{fi}(t) = \frac{\hbar\omega_2\omega_1^2}{4\varepsilon_2\varepsilon_1^2}|\chi^{(2)}\gamma_2|^2 n^2 t. \quad (32)$$

Hence the second harmonic mean photon number is

$$\langle n_2(t)\rangle_{\text{QM}} = \frac{\hbar\omega_2\omega_1^2}{16\varepsilon_2\varepsilon_1^2}|\chi^{(2)}\gamma_2|^2 n^2 t^2. \quad (33)$$

Comparing this expression to the classical calculation for energy time dependence of SHG, rewritten in terms of photon numbers

$$n_2(t)_{\text{classical}} = \frac{\hbar\omega_2\omega_1^2}{16\varepsilon_2\varepsilon_1^2}|\chi^{(2)}\gamma_2|^2 n_1^2 t^2, \quad (34)$$

proves the two models to be in good agreement at the classical limit according to the correspondence principle.

IV. SPONTANEOUS PHOTON CONVERSION CALCULATIONS

In a process of spontaneous 2PDC one pump photon is annihilated and two down-converted photons are created. In free-space interaction the down-conversion spectrum can be generally very broad [35]. However, in high-finesse cavities, only a discrete set of eigenmodes are allowed. We assume a specific cavity design such that the pump of the spontaneous PDC is tuned to one of the cavity eigenmodes, and the product degenerate PDC frequency is at another cavity eigenmode. Furthermore, the cavity is taken to be small (a few wavelengths) such that the free spectral range is large and no additional cavity eigenmode frequencies overlap the down-conversion spectrum. In general, complex photonic cavities can be designed for a specific nondegenerate PDC case; however, in the current example we treat only the degenerate case with $\omega_2=2\omega_1$.

Hence the initial and the final states are

$$|i\rangle = |n_{\omega_2},0_{\omega_1}\rangle,$$

$$|f\rangle = |n-1_{\omega_2},2_{\omega_1}\rangle. \quad (35)$$

This process can be viewed as a transition of a photon from a higher cavity eigenstate $2\omega_1$ to a lower cavity eigenstate ω_1 by emitting a ω_1 photon [Fig. 1(c)]. For 2PDC the only nonvanishing operator term of the scattering matrix $S^{(1)}$ is $a_{\omega_2}(a_{\omega_1}^\dagger)^2$ leaving

$$S_{fi}(t) = \frac{-i\chi^{(2)}}{2\hbar}\sqrt{\frac{\hbar\omega_2}{\varepsilon_2}}\left(\frac{\hbar\omega_1}{\varepsilon_1}\right)\int_{-\infty}^t dt' \int d\mathbf{r}\sqrt{2n}F_1(\mathbf{r}) \times[F_2^*(\mathbf{r})]^2 e^{2i\omega_1 t}e^{-i\omega_2 t}. \quad (36)$$

The spontaneous process is generally very weak and should be considered as a long-time interaction. The transition probability for $t<\infty$ is then

$$P_{fi}(t) = S_{fi}(t)^2 = \left(\frac{\hbar\omega_2}{\varepsilon_2}\right)\left(\frac{\hbar\omega_1}{\varepsilon_1}\right)^2\left|\frac{\chi^{(2)}}{2\hbar}\gamma_2\right|^2 2n\left|\frac{e^{i\Delta\omega t}-1}{\Delta\omega t}\right|^2 t^2, \quad (37)$$

where $\Delta\omega=\omega_2-2\omega_1$. Using energy conservation restriction $\Delta\omega=0$ the transition rate is

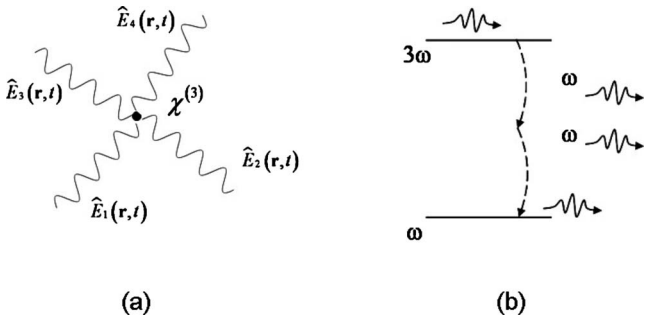

FIG. 2. (a) Four-photon vertex diagram for third-order nonlinear interaction. (b) Photon down-transition by two photon emission—3PDC.

$$R_{fi} = \frac{P_{fi}(t)}{t} = \frac{\hbar\pi}{\omega_2}\left(\frac{\omega_2}{\varepsilon_2}\right)\left(\frac{\omega_1}{\varepsilon_1}\right)^2 \left|\frac{\chi^{(2)}}{4}\gamma_2\right|^2 n_1. \tag{38}$$

Thus the pump photon lifetime for 2PDC process is

$$\tau_p^{\text{2PDC}} = \frac{1}{R_{fi}} = \frac{\omega_2}{\hbar\pi n_1}\left(\frac{\varepsilon_2}{\omega_2}\right)\left(\frac{\varepsilon_1}{\omega_1}\right)^2 \left|\frac{4}{\gamma_2\chi^{(2)}}\right|^2. \tag{39}$$

For a third-order nonlinear four-wave mixing process of 3PDC the interaction Hamiltonian density is

$$\hat{\mathcal{H}}_{\text{int}} = \frac{\chi^{(3)}}{2}\hat{E}_1(\mathbf{r},t)\hat{E}_2(\mathbf{r},t)\hat{E}_3(\mathbf{r},t)\hat{E}_4(\mathbf{r},t), \tag{40}$$

where $\chi^{(3)}$ is the third order nonlinear susceptibility, which is described by a four-photon vertex [Fig. 2(a)]. The scattering matrix S to the first order in the perturbation theory is

$$S^{(1)} = \frac{-i}{\hbar}\int dt\, H_{\text{int}} = \frac{-i\chi^{(3)}}{2\hbar}\int dt \int d\mathbf{r}\, \hat{E}_1(\mathbf{r},t)\hat{E}_2(\mathbf{r},t)\hat{E}_3(\mathbf{r},t)\hat{E}_4(\mathbf{r},t). \tag{41}$$

In a process of spontaneous 3PDC one pump photon is annihilated and three down-converted photons are created. Hence assuming a cavity designed to have resonances at the pump with ω_3 and at the degenerate downconversion $\omega_1 = \omega_3/3$ frequencies, the initial and the final states are

$$|i\rangle = |n_{\omega_3}, 0_{\omega_1}\rangle,$$

$$|f\rangle = |n-1_{\omega_3}, 3_{\omega_1}\rangle, \tag{42}$$

with n being the number of photons in the pump field. This process can be viewed as a transition of a photon from a higher state $3\omega_1$ to a lower cavity eigenstate ω_1 by emitting two ω_1 photons [Fig. 2(b)]. In 3PDC the only nonvanishing operator part of $S^{(1)}$ is $a_{\omega_3}(a^\dagger_{\omega_1})^3$ leaving

$$S_{fi(t)} = \frac{-i\chi^{(3)}}{2\hbar}\left(\sqrt{\frac{\hbar\omega_3}{\varepsilon_3}}\right)\left(\frac{\hbar\omega_1}{\varepsilon_1}\right)^{\frac{3}{2}}\sqrt{6n}\int_0^t dt' \int d\mathbf{r}\, F_1(\mathbf{r}) \times [F_2^*(\mathbf{r})]^3 e^{3i\omega_1 t'} e^{-i\omega_3 t'}. \tag{43}$$

For a weak long-time interaction the transition probability amplitude for $t\to\infty$ is then

$$S_{fi} = \frac{-i\chi^{(3)}}{2\hbar}\left(\sqrt{\frac{\hbar\omega_3}{\varepsilon_3}}\right)\left(\frac{\hbar\omega_1}{\varepsilon_1}\right)^{\frac{3}{2}}\sqrt{6n}\,\delta(3\omega_1-\omega_3), \tag{44}$$

where

$$\gamma_3 = \int d\mathbf{r}\, F_1(\mathbf{r})[F_2^*(\mathbf{r})]^3 \tag{45}$$

is the four-mode nonlinear overlap or momentum-conservation factor. The transition probability for $t<\infty$ using energy conservation restriction $\Delta\omega=0$ is

$$P_{fi} = \frac{\hbar^2 3\pi}{4\omega_3}\left|\frac{\chi^{(3)}}{2}\gamma_3\right|^2 n\left(\frac{\omega_3}{\varepsilon_3}\right)\left(\frac{\omega_1}{\varepsilon_1}\right)^3 t \tag{46}$$

and the corresponding pump photon lifetime in a 3PDC process is

$$\tau_p^{\text{3PDC}} = \frac{4\omega_3}{3\pi n\hbar^2}\left|\frac{2}{\chi^{(3)}\gamma_3}\right|^2\left(\frac{\varepsilon_3}{\omega_3}\right)\left(\frac{\varepsilon_1}{\omega_1}\right)^3. \tag{47}$$

Thus the 3PDC pump photon lifetime is longer than a 2PDC lifetime by a factor

$$\frac{\tau_p^{\text{3PDC}}}{\tau_p^{\text{2PDC}}} = \frac{1}{3\hbar}\left|\frac{\chi^{(2)}\gamma_2}{\chi^{(3)}\gamma_3}\right|^2\left(\frac{\varepsilon(\omega_{\text{3PDC}})}{\omega_{\text{3PDC}}}\right)^3\left(\frac{\omega_{\text{2PDC}}}{\varepsilon(\omega_{\text{2PDC}})}\right)^2. \tag{48}$$

For a degenerate case $\omega_{\text{3PDC1}}=\omega_p/3$ and $\omega_{\text{2PDC}}=\omega_p/2$

$$\frac{\tau_p^{\text{3PDC}}}{\tau_p^{\text{2PDC}}} = \frac{1}{3\hbar}\left|\frac{\chi^{(2)}\gamma_2}{\chi^{(3)}\gamma_3}\right|^2\left(\frac{3\varepsilon(\omega_{\text{3PDC}})}{\omega_p}\right)^3\left(\frac{\omega_p}{2\varepsilon(\omega_{\text{2PDC}})}\right)^2 = \frac{9}{4\omega_p\hbar}\left|\frac{\chi^{(2)}\gamma_2}{\chi^{(3)}\gamma_3}\right|^2\frac{\varepsilon^3(\omega_{\text{3PDC}})}{\varepsilon^2(\omega_{\text{2PDC}})}. \tag{49}$$

Assuming the same order of magnitude for dielectric constants at different wavelengths $\varepsilon(\omega_{\text{3PDC}})\sim\varepsilon(\omega_{\text{2PDC}})$ the conversion rate ratio is

$$\frac{R^{\text{2PDC}}}{R^{\text{3PDC}}} \sim \frac{\varepsilon}{E_p^{\text{ph}}}\left|\frac{\chi^{(2)}\gamma_2}{\chi^{(3)}\gamma_3}\right|^2, \tag{50}$$

which is the ratio between the second and the third order nonlinear interaction energies including dispersion, expressed in the units of the pump photon energy. This result demonstrates the crucial role of dispersion for cavity spontaneous photon conversion processes, which can be manipulated by the spatial mode modification determined by the cavity design.

V. SPDC RATE CALCULATIONS IN DISPERSIVE CAVITIES

The effect of one-dimensional cavity length with dispersive mirrors on nonlinear process efficiency has been calcu-

lated classically for a constant wavelength relative to a given material resonance [24] and shown experimentally for standing-wave SHG [36]. We use our quantum formalism in order to calculate the spontaneous photon down-conversion rate dependence on the cavity dimensions and the wavelength, taking into consideration dispersion and nonlinearity due to a close material resonance. It is important to discriminate between the two types of resonances in the presented examples: The optical cavity resonances that comprise the eigenmode set, and the material transition resonances that determine the dispersion and the nonlinear coefficients. In the following all the nonlinear processes occur at frequencies that are cavity eigenmodes and thus the analysis relates to pump and product frequencies that match cavity eigenmodes. However, the material transition resonance, ω_{res}, is detuned in general from the cavity eigenmode frequency, and this detuning can be changed for example by changing the nonlinear material under discussion.

For a single atomic resonance the linear susceptibility [33] is

$$\chi_{ij}^{(1)}(\omega) = \frac{1}{\hbar}\left[\frac{\mu_{ge}^{i}\mu_{eg}^{j}}{(\omega_{eg}-\omega)}\right] \tag{51}$$

and the refractive index is

$$n(\omega) = \sqrt{1+\text{Re}[\chi_{ij}^{(1)}(\omega)]} = \sqrt{1+\text{Re}\left(\frac{1}{\hbar}\left[\frac{\mu_{ge}^{i}\mu_{eg}^{j}}{(\omega_{eg}-\omega)}\right]\right)}, \tag{52}$$

where $\omega_{\text{eg}}=\omega_{\text{res}}$ is the material ground-to-excited level resonance frequency and μ_{eg} is the dipole moment. The pump is assumed to be strong enough to be constant in time, and for the down-converted photons the only material loss mechanism is due to two-photon absorption and thus can be neglected. The nonlinear second-order susceptibility is given by

$$\chi_{ijk}^{(2)}(\omega_1+\omega_2,\omega_1,\omega_2) = \frac{1}{\hbar^2}\left[\frac{\mu_{ge}^{i}\mu_{em}^{j}\mu_{mg}^{k}}{(\omega_{ge}-\omega_1-\omega_2)(\omega_{mg}-\omega_2)}\right], \tag{53}$$

where $\omega_1+\omega_2$, ω_1,ω_2 are the optical pump and the product frequencies, $\omega_{\text{eg}}=\omega_{\text{res}}$ is the material transition frequency, and m is a virtual level.

Dispersion is expected to become larger close to the material resonance thus reducing the phase-matching efficiency [Eq. (52)], while the nonlinear coefficient grows as well towards the resonance frequency [Eq. (53)] thus increasing the local process efficiency. The overall nonlinear process efficiency should therefore have an optimum considering these contradicting tendencies of the local effect and the phase matching. Very high Q photonic crystal cavities can be realized with defect resonances at the pump and the downconverted photon frequencies. In a one-dimensional cavity the photonic crystal defect design for a standing wave mode is in fact equivalent to dispersive reflector design for traveling wave phase matching [24], due to the different effective cavity lengths of the interacting frequencies providing the different phases. The localized standing wave spatial dependence inside the cavity is

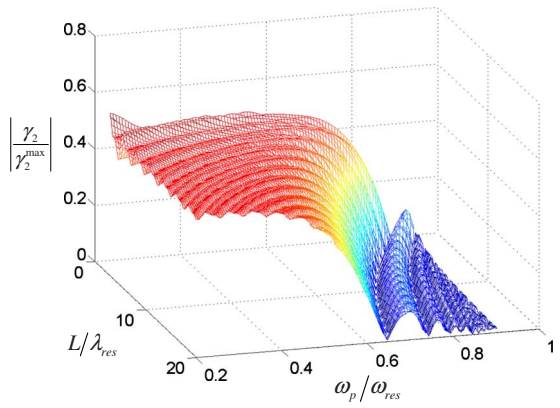

FIG. 3. (Color online) Normalized 2PDC phase-matching term vs pump frequency in units of ω_{res} and cavity size in units of λ_{res} ("res" denotes the material resonance).

$$F(\mathbf{r},\omega) = \cos[k_x(\omega)x], \tag{54}$$

with the dispersion relation

$$k_x(\omega) = n(\omega)\omega\sqrt{\mu\varepsilon_0}. \tag{55}$$

For very high-Q cavity the contribution of the exponentially decaying field outside the cavity can be neglected and thus the phase-matching term for 2PDC is

$$\gamma_2 = \int_{-\frac{L}{2}}^{\frac{L}{2}} \cos[k_x(2\omega)x]\cos^2[k_x(\omega)x]dx, \tag{56}$$

where L is the cavity length. Performing the x integration yields

$$\gamma_2 = \frac{\sin\left(\Delta k\frac{L}{2}\right)}{2\Delta k} + \frac{1}{2}\left(\frac{\sin\left(q\frac{L}{2}\right)}{q} + \frac{2\sin\left(k_x(2\omega)\frac{L}{2}\right)}{k_x(2\omega)}\right), \tag{57}$$

where $\Delta k=k_x(2\omega)-2k_x(\omega)$ and $q=k_x(2\omega)+2k_x(\omega)$.

Calculations of the phase-matching term γ_2 were performed for different values of the cavity length and pumping frequency. The pump frequency in Figs. 3–6 is normalized to the material transition resonant frequency, ω_{res}, and the length of the cavity is given in units of resonant material wavelength, λ_{res}. The plot of the calculated phase-matching term γ_2 is normalized to the ideal phasematching case $\gamma_{\max}$, where all the spatial modes in the nonlinear interaction are identical, equivalent to the zero-dispersion case in the traveling wave nonlinear interaction. The detailed structure of the phase-matching dependence on the cavity size and pump frequency is determined by the different terms in Eq. (57). The main contribution to the phase matching is due to the first term, that is inversely proportional to the dispersion-induced phase mismatch Δk; the latter is generally much smaller than k_x making this term the dominant one. For a

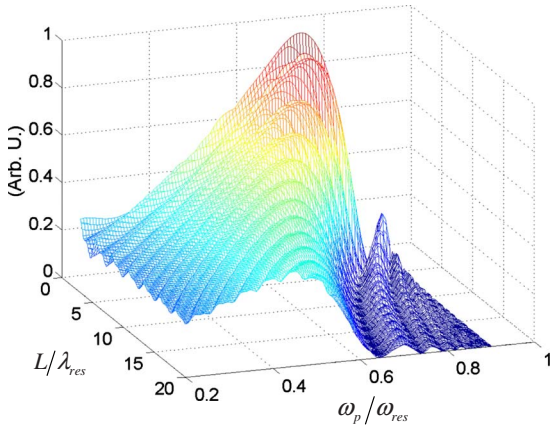

FIG. 4. (Color online) Normalized 2PDC rate vs pump frequency in units of ω_{res} and cavity size in units of λ_{res} ("res" denotes the material resonance).

constant pump frequency this term contributes the slowest oscillation (Fig. 3) with oscillation period equal to the nonlinear coherence length L_c, while for a constant cavity length, increasing the pump frequency results in stronger dispersion (larger Δk) and thus yields slow oscillations with decreasing periods. The additional terms in Eq. (57) contribute much smaller oscillations $[\sim 1/2k_x(\omega)]$ with much shorter periods ($\sim$ one pump wavelength), whereas the exact form of these fast oscillations is determined by the Fourier series coefficients of these two higher harmonics of $k_x(\omega)$. The calculations show a stronger mismatch for pump frequencies closer to the material resonance due to the higher dispersion which deteriorates the phasematching and for larger cavity lengths (Fig. 3). However, the high dispersion close to the resonance frequency is accompanied by larger nonlinearity and thus the overall 2PDC process efficiency has a definite maximum, which is located at lower frequencies for larger cavities (Fig. 4).

In the 3PDC process the nonlinear third-order susceptibility, with $\omega_1+\omega_2+\omega_3, \omega_1, \omega_2, \omega_3$ optical pump and product frequencies, $\omega_{\mathrm{eg}}=\omega_{\mathrm{res}}$, the resonant transition frequency, and n, m virtual levels, is

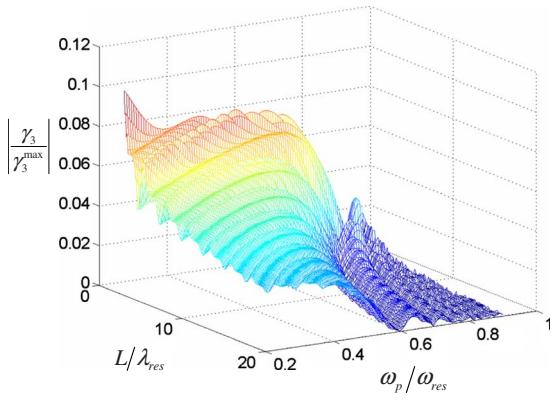

FIG. 5. (Color online) Normalized 3PDC phase-matching term vs pump frequency in units of ω_{res} and cavity size in units of λ_{res} ("res" denotes the material resonance).

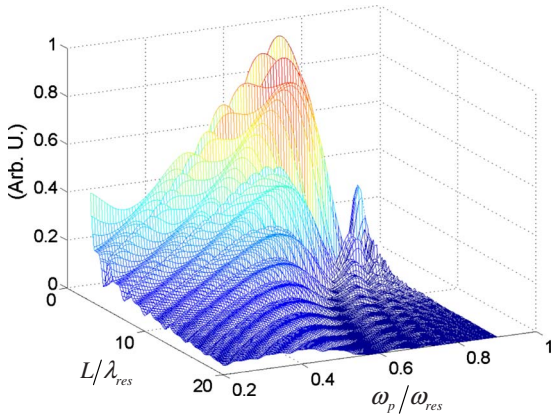

FIG. 6. (Color online) Normalized 3PDC rate vs pump frequency in units of ω_{res} and cavity size in units of λ_{res} ("res" denotes the material resonance).

$$\chi^{(3)}_{ijkh}(\omega_1+\omega_2+\omega_3,\omega_1,\omega_2,\omega_3) = \frac{1}{\hbar^3}\left[\frac{\mu^h_{ge}\mu^i_{ge}\mu^j_{em}\mu^k_{mg}}{(\omega_{ng}-\omega_3)(\omega_{ge}-\omega_1-\omega_2)(\omega_{mg}-\omega_2)}\right], \quad (58)$$

whereas the phase-matching term for 3PDC is

$$\gamma_3 = \int_{-\frac{L}{2}}^{\frac{L}{2}} \cos[k_x(3\omega)x]\cos^3[k_x(\omega)x]dx \quad (59)$$

yielding after integration

$$\gamma_3 = \frac{\sin\left(\Delta k'\frac{L}{2}\right)}{4\Delta k'} + \frac{1}{4}\left(\frac{\sin\left(\kappa\frac{L}{2}\right)}{\kappa} + \frac{3\sin\left(\delta\frac{L}{2}\right)}{\delta} + \frac{3\sin\left(\sigma\frac{L}{2}\right)}{\sigma}\right), \quad (60)$$

where $\Delta k' = k_x(3\omega) - 3k_x(\omega)$, $\kappa = k_x(3\omega) + 3k_x(\omega)$, $\delta = k_x(3\omega) - k_x(\omega)$, and $\sigma = k_x(3\omega) + k_x(\omega)$.

Similar to the 2PDC case, in 3PDC the main contribution to γ_3 is due to the first term in Eq. (60). For a constant ω_p this term contributes the slowest oscillation (Fig. 5), with oscillation period L_c shorter than that of 2PDC due to the larger difference between the pump and the product frequencies. The additional terms in Eq. (60) contribute much smaller oscillations with about one pump wavelength periods, while the exact oscillation form is determined by the Fourier coefficients of these three higher harmonics of $k_x(\omega)$.

The 3PDC phase-matching term γ_3 exhibits even stronger dependence on the cavity length and the pumping frequency (Fig. 5) than γ_2, and the overall 3PDC efficiency decays very rapidly with increased cavity size (Fig. 6) causing the optimal cavity length to be no larger than a few free-space wavelengths, which is close to the coherence length L_c in the design of QPM nonlinear optics.

VI. CONCLUSION

We have developed a simple phenomenological quantum-field model for the nonlinear process of photon frequency conversion in dispersive dielectric microcavities allowing practical calculations of conversion rates and efficiency optimization. The model incorporates the effect of dispersion into the structure of spatial cavity eigenmodes, while the material properties enter the calculations only through the dielectric constant spatial dependence and the nonlinear coupling coefficients. The nonlinear interaction between photonic cavity eigenmodes resembles atomic transition between electron eigenmodes and thus simple expressions for photon-to-photon decay rates are achieved for cavity stimulated and spontaneous photon conversion processes. The model is validated by comparing the stimulated SHG in the high-photon number limit to the classical time-dependant calculation in the slow time-varying envelope approximation, equivalently to the time-dependent perturbation theory assumptions in the quantum-field calculation. We show that in a cavity nonlinear process the phase-matching requirement translates into a nonlinear mode overlap manifesting the momentum-conservation in a k space spanned by the cavity modes. We derive the expressions for the 2PDC and 3PDC photon lifetimes and the ratio between the conversion rates of both processes, which is the ratio between the second and the third order nonlinear interaction energies including dispersion, expressed in the units of the pump photon energy. This result demonstrates the necessity for proper engineering of the spatial mode by the cavity design in order to overcome material dispersion effect on cavity spontaneous photon conversion processes.

To illustrate the effectiveness of the developed formalism we analyzed degenerate 2PDC and 3PDC rates in a dispersive cavity. Taking for concreteness the material properties as determined by a discrete-level atomic system we calculate the spontaneous photon down-conversion rate dependence on the cavity dimensions and the wavelength taking into consideration dispersion and nonlinearity dependence close to material resonance, while always assuming the cavity eigenmodes to match the nonlinear interaction frequencies. Calculations of the phase-matching terms γ_2 and γ_3 for different values of the cavity length and pumping frequency show a higher mismatch for pump frequencies closer to the resonance due to the stronger dispersion and for larger cavity lengths. However, due to larger nonlinearity near the resonance the overall process efficiency has a definite maximum located at lower frequencies for larger cavities.

[1] A. L. Migdall, D. Branning, and S. Castelletto, Phys. Rev. A **66**, 053805 (2002).
[2] E. Jeffrey, N. A. Peters, and P. G. Kwiat, New J. Phys. **6**, 100 (2004).
[3] T. B. Pittman, B. C. Jacobs, and J. D. Franson, Phys. Rev. A **66**, 042303 (2002).
[4] C. A. Holmes, G. J. Milburn, and D. F. Walls, Phys. Rev. A **39**, 2493 (1989).
[5] E. Waks, E. Diamanti, and Y. Yamamoto, New J. Phys. **8**, 4 (2006).
[6] A. Hayat and M. Orenstein, Appl. Phys. Lett. **89**, 171108 (2006).
[7] M. W. Mitchell, J. S. Lundeen, and A. M. Steinberg, Nature (London) **429**, 161 (2004).
[8] K. J. Resch, J. L. O'Brien, T. J. Weinhold, K. Sanaka, and A. G. White, Phys. Rev. Lett. **98**, 203602 (2007).
[9] P. G. Kwiat, K. Mattle, H. Weinfurter, A. Zeilinger, A. V. Sergienko, and Y. Shih, Phys. Rev. Lett. **75**, 4337 (1995).
[10] J. Jing, S. Feng, R. Bloomer, and O. Pfister, Phys. Rev. A **74**, 041804(R) (2006).
[11] J-W. Pan, D. Bouwmeester, H. Weinfurter, and A. Zeilinger, Phys. Rev. Lett. **80**, 3891 (1998).
[12] A. K. Ekert, J. G. Rarity, P. R. Tapster, and G. Massimo Palma, Phys. Rev. Lett. **69**, 1293 (1992).
[13] C. H. Bennett, G. Brassard, C. Crépeau, R. Jozsa, A. Peres, and W. K. Wootters, Phys. Rev. Lett. **70**, 1895 (1993).
[14] K. Mattle, H. Weinfurter, P. G. Kwiat, and A. Zeilinger, Phys. Rev. Lett. **76**, 4656 (1996).
[15] A. Einstein, B. Podolsky, and N. Rosen, Phys. Rev. **47**, 777 (1935).
[16] J. F. Clauser, M. A. Horne, A. Shimony, and R. A. Holt, Phys. Rev. Lett. **23**, 880 (1969).
[17] J. Douady and B. Boulanger, Opt. Lett. **29**, 2794 (2004).
[18] K. Banaszek and P. L. Knight, Phys. Rev. A **55**, 2368 (1997).
[19] T. Felbinger, S. Schiller, and J. Mlynek, Phys. Rev. Lett. **80**, 492 (1998).
[20] D. M. Greenberger, M. A. Horne, A. Shimony, and A. Zeilinger, Am. J. Phys. **58**, 1131 (1990).
[21] K. Banaszek, A. B. U'Ren, and I. A. Walmsley, Opt. Lett. **26**, 1367 (2001).
[22] L. Lanco, S. Ducci, J. P. Likforman, X. Marcadet, J. A. W. van Houwelingen, H. Zbinden, G. Leo, and V. Berger, Phys. Rev. Lett. **97**, 173901 (2006).
[23] D. Artigas, E. U. Rafailov, P. Loza-Alvarez, and W. Sibbett, IEEE J. Quantum Electron. **40**, 1122 (2004).
[24] G. Klemens, C. -H. Chen, and Y. Fainman, Opt. Express **13**, 9388 (2005).
[25] Z. Yang, P. Chak, A. D. Bristow, H. M. van Driel, R. Iyer, J. S. Aitchison, A. L. Smirl, and J. E. Sipe, Opt. Lett. **32**, 826 (2007).
[26] Z. Y. Ou and Y. J. Lu, Phys. Rev. Lett. **83**, 2556 (1999).
[27] Bruno Huttner and Stephen M. Barnett, Phys. Rev. A **46**, 4306 (1992).
[28] R. J. Glauber and M. Lewenstein, Phys. Rev. A **43**, 467 (1991).
[29] P. D. Drummond, Phys. Rev. A **42**, 6845 (1990).
[30] M. Hillery and L. D. Mlodinow, Phys. Rev. A **30**, 1860 (1984).
[31] T. A. B. Kennedy and E. M. Wright, Phys. Rev. A **38**, 212 (1988).

[32] A. Yariv, *Optical Electronics in Modern Communications* (Oxford University Press, New York, 1997).
[33] R. Boyd, *Nonlinear Optics*, 2nd ed. (Academic Press, New York, 2003).
[34] F. Mandl and G. Shaw, *Quantum Field Theory* (John Wiley & Sons, New York, 1984).
[35] K. A. O'Donnell and A. B. U'Ren, Opt. Lett. **32**, 817 (2007).
[36] A. Hayat and M. Orenstein, Opt. Lett. **32**, 2864 (2007)